

# Numerical study on Brazilian test of slate with different bedding orientations

**Bing Xie<sup>1, 2\*</sup> Yunling Ma<sup>2</sup>, Wuxiu Ding<sup>2</sup>**

<sup>1</sup>Luoyang Institute of Hydraulic Engineering and Technology, Luoyang, 470123, Henan, China

<sup>2</sup>Civil Engineering Department, Luoyang Institute of Science and Technology, Luoyang, 471003, Henan, China

Received 20 October 2014, www.cmnt.lv

## Abstract

There are a variety of parallel planes of weakness in slate; consequently, slate's tensile strength can be significantly impacted by different bedding orientations in the weak planes. In order to reveal the anisotropy of tensile strength and difference between the fracture patterns caused by the orientation of weak planes, Brazilian tests were carried out using numerical specimens with ten types of bedding angles by implementing a discrete element method. The anisotropy of tensile strength and fracture patterns were obtained through a series of simulations; the results shows that there are three kinds of failure forms in the specimens, which are as follows: a pure tensile failure when the bedding angle was , a shearing failure when the bedding angle was , and a mixed failure mode when the bedding angle was between 40° and 70°.

*Keywords:* Tensile strength; Fracture pattern; Brazilian test; Discrete elements

## 1 Introduction

Bedding is the primary feature of slate and can be divided into three categories according to its shape: horizontal bedding, vertical bedding and inclined bedding. Usually, slate shows obvious anisotropy due to differences in the direction of slate components or mineral interlayer composition, and the tensile strength of the slate is directionally dependent, as opposed to isotropic rock that implies identical properties in all directions.

A great deal of research has been conducted on tensile strength and fracture patterns in the slate, and a number of important conclusions have been achieved. For example, through a combination of analytical and experimental methods Chen [1] obtained the indirect tensile strength of anisotropic media from the failure loads measured during diametral loading. Debecker [2] performed a series of loading tests on circular samples to examine fracture patterns in slate, and found that the strength anisotropy on  $\mu$ -scale is the key factor behind the strength anisotropy on sample scale. Tavallali [3] studied the effects of the layer orientation on failure strength and fractures induced by the Brazilian tensile test, specific to one particular sandstone from Modave in the South of Belgium; the variation in the strength and the applied energy were examined as a function of the inclination angle between the layer plane and the loading direction. There are many similar studies, including paper [4-7]. In almost all of the literature mentioned above, the anisotropy of tensile strength or the failure patterns in slate were studied from theoretical and experimental points of view; however, little attention was paid to the crack propagation process at the mesoscopic level in the test. A numerical simulation of the Brazilian test on slate will be carried out here at the mesoscopic level so that the anisotropy of the tensile strength and the propagation and expansion of cracks can be analyzed.

## 2 Calculation Principle of PFC2D

The choice in this study is the numerical code PFC2D, 2D discrete element software, developed by the Itasca Company; it is able to model a brittle solid by bonding every particle to its neighbor. The resulting assembly can be regarded as "rock" and is capable of "fracturing" when bonds break in a progressive manner.

PFC2D contains the following assumptions: the particles are treated as rigid bodies; the contacts occur over a vanishingly small area; behavior at the contacts uses a soft-contact approach, wherein the rigid particles are allowed to overlap one another at contact points; the magnitude of the overlap is related to the contact force via the force displacement law, and all overlaps are small in relation to particle sizes; bonds can exist at contacts between particles; all particles are circular.

The calculation cycle in PFC2D is a timestepping algorithm that consists of the repeated application of the law of motion to each particle, a force-displacement law applied to each contact, and a constant updating of wall positions. Contacts, which may exist between two balls or between a ball and a wall, are formed and broken automatically during the course of a simulation. The calculation cycle is illustrated in Figure 1.

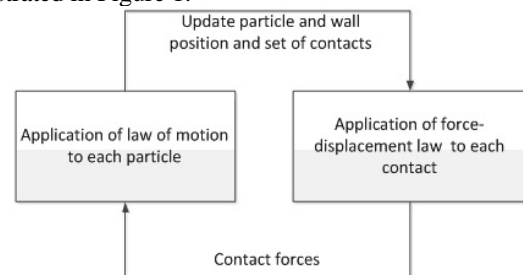


FIGURE 1 Calculation cycle in PFC2D

\* Corresponding author e-mail: rs425@126.com

The overall constitutive behavior of rock material can be simulated in PFC2D by associating a simple constitutive model of the parallel bond at each contact, which can transmit both force and moment[8]. It is shown in Figure 2[9] that the total force and moment associated with the parallel bond are denoted by  $\bar{F}_i$  and  $\bar{M}_3$ .

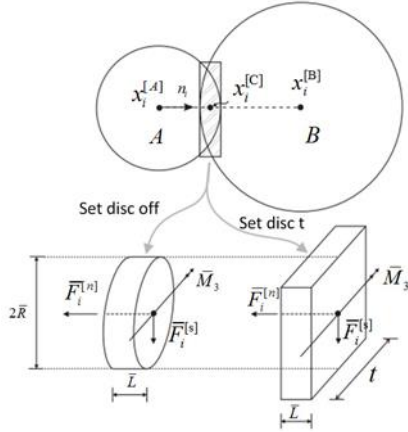


FIGURE 2 Sketch of parallel bond

The force vector can be resolved into normal and shear components with respect to the contact plane as:

$$\bar{F}_i = \bar{F}_i^n + \bar{F}_i^s, \tag{1}$$

where  $\bar{F}_i^n$  and  $\bar{F}_i^s$  denote the normal and shear component vectors, respectively.

The normal force component vector can be expressed in terms of the scalar value,  $\bar{F}^n$ , via

$$\bar{F}_i^n = (\bar{F}_j^n n_j) n_i = \bar{F}^n n_i. \tag{2}$$

When the bond is formed,  $\bar{F}_i$  and  $\bar{M}_3$  are initialized to zero. Each subsequent relative displacement and rotation-increment at the contact results in an increment of elastic force and moment, which is then added to the current values. The elastic force increments occurring over a time step of  $\Delta t$  are calculated using:

$$\Delta \bar{F}_i^n = (-\bar{k}^n A \Delta U^n) n_i, \tag{3}$$

$$\Delta \bar{F}_i^s = -\bar{k}^s A \Delta U_i^s, \tag{4}$$

with  $\Delta U_i = V_i \Delta t$  and the moment increment is calculated using:

$$\Delta \bar{M}_3 = -\bar{k}^m I \Delta \theta_3, \tag{5}$$

with  $\Delta \theta_3 = (\omega_3^{[B]} - \omega_3^{[A]}) \Delta t$ , where  $V_i$  is the contact velocity, A is the area of the bond cross-section; and I is the moment of inertia in the bond cross-section with an axis through the contact point in the direction of  $\Delta \theta_3$ .

The new force and moment vectors associated with the parallel bond were found by adding the old values existing at the beginning of the time step to the elastic force- and moment-increment vectors. The new force vectors are calculated by:

$$\bar{F}_i^n \leftarrow \bar{F}_i^n + \Delta \bar{F}_i^n, \tag{6}$$

$$\bar{F}_i^s \leftarrow \bar{F}_i^s + \Delta \bar{F}_i^s \tag{7}$$

and the new moment vector is calculated by:

$$\bar{M}_3 \leftarrow \bar{M}_3 + \Delta \bar{M}_3. \tag{8}$$

The maximum tensile and shear stresses acting on the bond periphery are calculated to be:

$$\sigma_{\max} = \frac{-\bar{F}_i^n}{A} + \frac{|\bar{M}_3|}{I} \bar{R}, \tag{9}$$

$$\tau_{\max} = \frac{|\bar{F}_i^s|}{A}, \tag{10}$$

If the maximum tensile stress exceeds the normal strength ( $\sigma_{\max} \geq \bar{\sigma}_c$ ) or the maximum shear stress exceeds the shear strength ( $\tau_{\max} \geq \bar{\tau}_c$ ), then the parallel bond breaks.

### 3 Verification of calculating using PFC2D

In order to verify the accuracy of the calculations in PFC2D, a numerical specimen of slate for the Brazilian test has been established in Fig.3. The difference in the Brazilian test results between numerical simulation and theoretical analysis could then be analyzed in the instance of being without bedding structures.

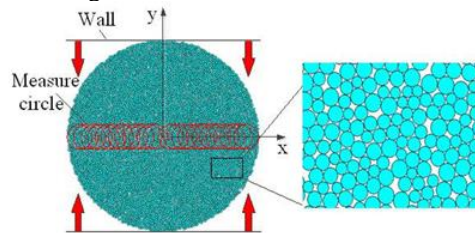


FIGURE 3 Sketch of Brazilian test of numerical specimen without bedding

The numerical specimen contains more than 8000 particles with a diameter of 50 mm. Here, the parallel bonding model has been employed for particle contact. Two rigid walls have been set at the top and bottom of the specimen as loading platens; the velocities of walls can be controlled using a servomechanism for steady loading. As shown in Fig. 3, twenty-four measurement circles have been set along the O-x direction in the center of the specimen to measure the stress and strain at the corresponding positions. Mesoscopic parameters of particles and the parallel-bond can be seen in Tab. 1

TABLE 1 Meso properties of particles and the parallel-bond

Type	Micro-property	Value	Unit
Particle properties	Particle density	2630	kg m <sup>-3</sup>
	Young's modulus	30e9	Pa
	Friction coefficient	0.5	—
Parallel bond properties	Young's modulus	30e9	Pa
	Normal to shear stiffness ratio	1.8	—
	Normal strength	32e6	Pa
	Normal strength standard deviation	8e6	Pa
	Shear strength	20e6	Pa
	Shear strength standard deviation	5e6	Pa

Fig. 4 shows the force-strain curves and the distribution of cracks for the numerical specimens at the end of the loading process. The tensile strength of specimens was obtained from the simulation; it was 5.4 MPa. The stress and strain at each measure circle also can be obtained at the same time.

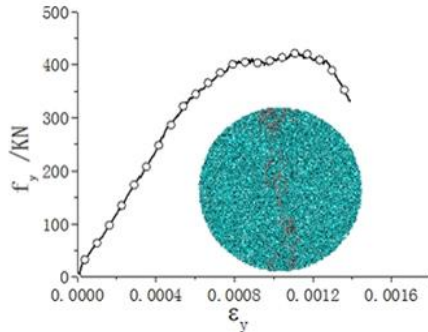


FIGURE 4 Result of Brazilian test of numerical specimen specimen without bedding

An analytic solution for a pair of diametrically opposed, symmetric and compressive line loads applied on an isotropic Brazilian disc were provided by Ye[10]. The solution for an isotropic Brazilian disc subjected to concentrated loads is:

$$\sigma_x = \frac{2P}{\pi l} \left[ \frac{((D/2)-y)x^2}{(((D/2)-y)^2 + x^2)^2} + \frac{((D/2)+y)x^2}{(((D/2)+y)^2 + x^2)^2} - \frac{1}{D} \right], \quad (11)$$

$$\sigma_y = \frac{2P}{\pi l} \left[ \frac{((D/2)-y)x^3}{(((D/2)-y)^2 + x^2)^2} + \frac{((D/2)+y)x^3}{(((D/2)+y)^2 + x^2)^2} - \frac{1}{D} \right], \quad (12)$$

$$\tau_{xy} = \frac{2P}{\pi l} \left[ \frac{((D/2)-y)^2 x}{(((D/2)-y)^2 + x^2)^2} + \frac{((D/2)+y)^2 x}{(((D/2)+y)^2 + x^2)^2} - \frac{1}{D} \right], \quad (13)$$

where P is the line load applied, l is the thickness of the disc, D is the diameter of the disc, and the rectangular coordinate system O-x-y is the same as in Figure 3.

Assuming y=0 in formulas (11), (12), and (13), the stress state on the diameter in O-x direction can be obtained as the following expression:

$$\begin{cases} \sigma_x = \frac{2P}{\pi D l} \left[ \frac{16D^2 x^2}{(4x^2 + D^2)^2} - 1 \right] \\ \sigma_y = \frac{2P}{\pi D l} \left[ \frac{4D^4}{(4x^2 + D^2)^2} - 1 \right] \\ \tau_{xy} = 0 \end{cases} \quad (14)$$

According to equation (14), an image of the function can be drawn when  $-0.25 \leq x \leq 0.25$ . If the calculation results from the measurement circle can also be plotted in the function image, Fig.5 can be drawn.

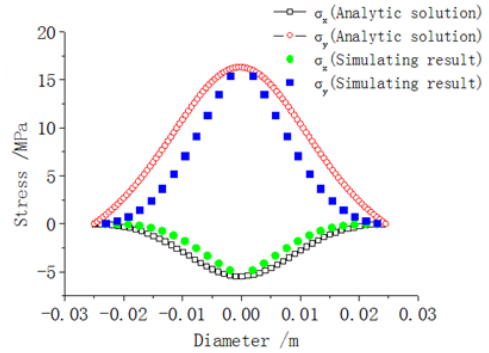


FIGURE 5 Comparison of calculated results

The calculation shows that the results of the Brazilian test for PFC2D and the theoretical analysis have good consistency. The calculation accuracy for PFC2D for Brazilian test is quite high.

#### 4 Brazilian test of slate using PFC2D

##### 4.1 TENSILE STRENGTH OF SLATE WITH DIFFERENT BEDDING

Slate is a layered rock that is at its weakest along its schistosity direction, also called cleavage direction or foliation. Slate is derived as a result of the low-grade metamorphosis of sedimentary shale. Also referred to as phyllite, it is the result of a certain degree of metamorphism between slate and mica schist [11].

In order to establish the feature of slate, weak contacts are used to simulate the bedding; a sketch of the model is shown in Figure 6.

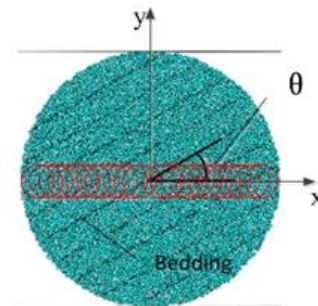


FIGURE 6 Numerical specimen of slate

The inclination angle of the bedding is  $\theta$ , and it is set as  $0^\circ, 10^\circ, 20^\circ, 30^\circ, 40^\circ, 50^\circ, 60^\circ, 70^\circ, 80^\circ$  and  $90^\circ$  respectively. The arrangement of measurement circles is the same as is shown in Fig. 3. Meso properties of bedding are shown in Tab. 2.

TABLE 2 Meso properties of bedding

Micro-property	Value	Unit
Friction coefficient	0.3	—
Normal strength	7e6	Pa
Shear strength	2e6	Pa
spacing	0.005	m

An approximate formula for the principal tension at the disc center (0,0) was derived from the analytical solution provided by Claesson [12], which represents the tensile strength of anisotropic rocks. Its form is as follows:

$$\sigma_{pr}(0,0) \cong \frac{P}{\pi Rl} \left[ \left( \sqrt[4]{E/E'} \right)^{\cos(2\theta_b)} - \frac{\cos(4\theta_b)}{4} (b-1) \right], \quad (15)$$

where

$$b = \frac{\sqrt{EE'}}{2} \left( \frac{1}{G'} - \frac{2\nu'}{E'} \right), \quad (16)$$

where the modulus of elasticity and Poisson's ratio are  $E$  and  $\nu$  in the  $x$ -direction. The applied load is  $P$ , and radius and thickness of disc are  $R$  and  $l$ , respectively. The corresponding quantities in the transverse  $y$ -direction are  $E'$  and  $\nu'$ . The modulus of shear is  $G'$  (Fig. 7). The angle between the direction of the applied force and the normal to the plane of transverse isotropy is  $\theta_i$ .

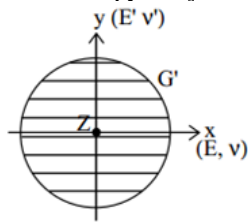


FIGURE 7 Brazilian test for an anisotropic material [12]

While the precision of the analytical solution for Brazilian test problems is high, the format of the equations is more complex. For specific problems if the exact solution is to be obtained, more calculation and experiments should be performed. Consequently, this paper uses the conventional formula for calculating tensile strength ( $\sigma_t$ ) according to the ISRM's recommendation [13]; see equation (17). This is further elaborated in other research on the tensile strength of layered rock in papers [3, 14-16].

Here, equation (17) is actually the result obtained from equation (11) while  $x=0$  and  $y=0$ , and the meaning of each parameter in equation (17) are same as equation (11).

$$\sigma_x = -\frac{2P}{\pi Dl}. \quad (17)$$

Calculated using PFC2D in accordance with equation (17), the results can be obtained as shown in Table 3.

TABLE 3 Results of numerical tests

Angle	$\sigma_t$ /MPa
0	5.09
10	4.81
20	4.01
30	3.71
40	2.70
50	2.33
60	2.15
70	2.01
80	1.91
90	1.71

It can be determined from Tab. 3 that as the changes from  $0^\circ$  to  $90^\circ$ , the tensile strength decreases gradually.

According to Table 3, variation trend of tensile strength that has been caused by the change of the bedding angle can be plotted in Fig. 8. From this it can be clearly observed that the tensile strength of slate has a significant nonlinear correlation with the bedding angle.

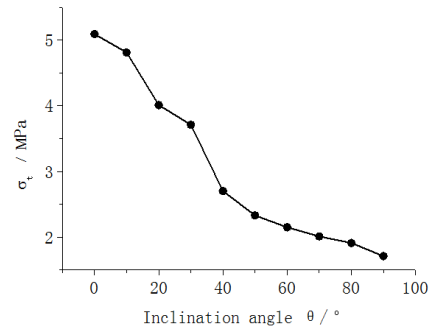


FIGURE 8 Tensile strength of specimen with different bedding angles

#### 4.2 CRACK PROPAGATION AND FAILURE OF THE BRAZILIAN TEST UNDER DIFFERENT BEDDING CONDITIONS

As mentioned before, if the contact stress of the particles in the numerical specimen generated by PFC2D exceeds its limits, the bond between the particles will break.

The break can be marked as a crack and that crack can also be distinguished as a normal crack or a shear crack according to that whether the crack has been caused by normal force or shear force, see Fig. 9.

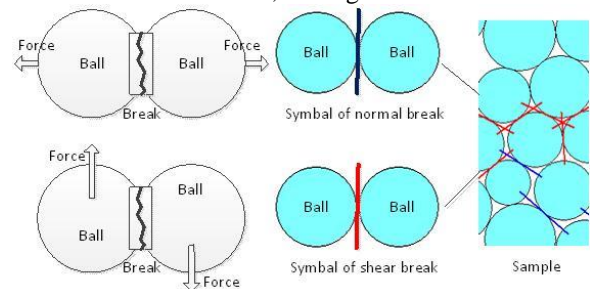


FIGURE 9 Sketch of marking cracks

If the propagation of the crack was marked during the entire loading process of the numerical Brazilian test, the visualized evolution of the rupture in the specimen can then be realized. The typical crack propagation process of specimens in the Brazilian test is shown in Fig. 10; here  $\theta = 30^\circ$ .

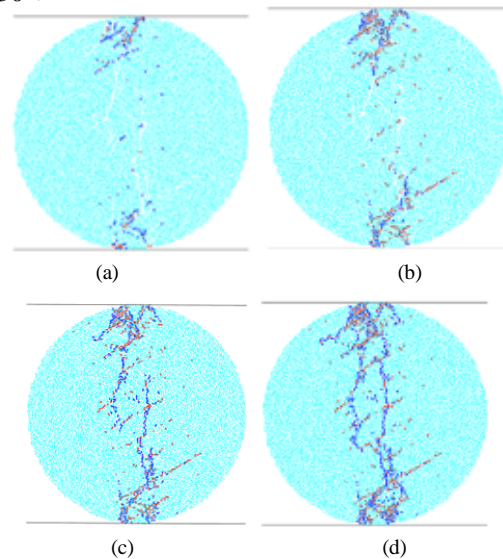


FIGURE 10 Process of crack propagation of specimen when  $\theta = 30^\circ$

From Fig. 10, it can be observed that although the shear cracks appeared between the layers, they were not connected, and the damage of the specimen was still caused by tension along the O-y direction.

Similarly, as shown in Fig. 11, the final state of the specimens with different bedding angles in Brazilian test can be obtained.

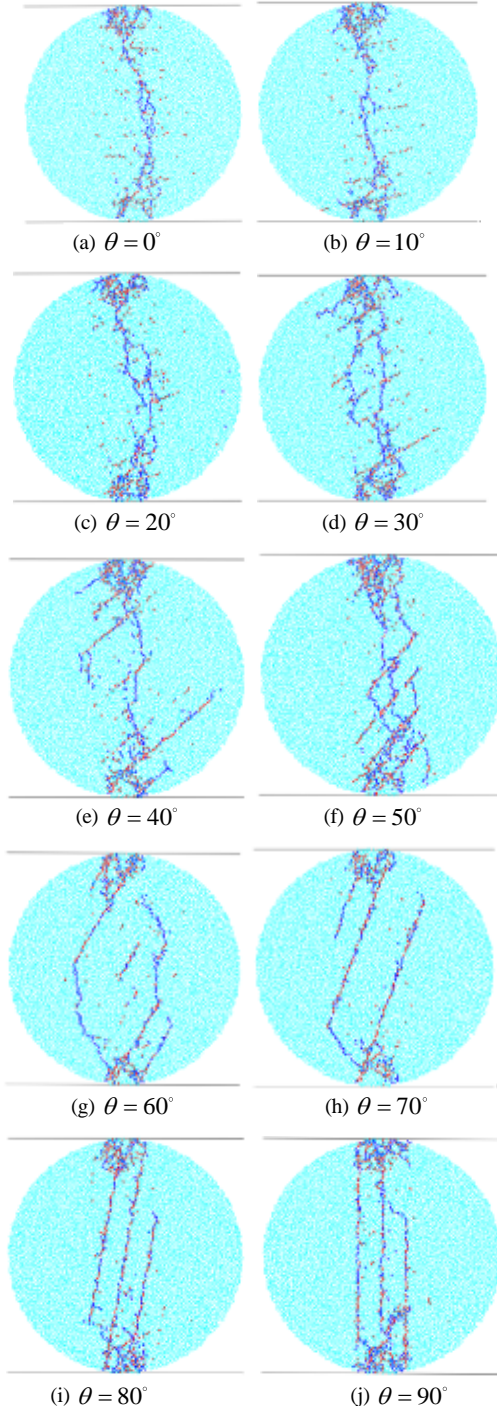


FIGURE 11 Final state of the numerical test in different bedding angle

The reasons for the formations shown in Fig. 11 are due to a lower normal strength and shear strength as well as a value of the friction coefficient at contacts in a layered position, which reflects natural layered rock conditions. Therefore, in the Brazilian test, as the bedding angle

increases, the failure type of the particle contact at the layer position will gradually change from normal to shear; a lower value of the friction coefficient for particle contact in a layered position will also cause dislocation between layers.

In order to conduct a quantitative analysis for cracks in the specimens, the total number of normal cracks and shear cracks must be counted and the statistic of percentages for different types of cracks must also be calculated. The results can be found in Tab. 4.

TABLE 4 Statistics of cracks

Angle/°	Normal crack		Shear crack		Total crack
	Number	Percentage	Number	Percentage	
0	432	59%	302	41%	734
10	398	53%	350	47%	748
20	342	48%	378	53%	720
30	322	45%	386	55%	708
40	320	44%	414	56%	734
50	292	39%	456	61%	748
60	198	30%	464	70%	662
70	182	27%	490	73%	672
80	174	26%	498	74%	672
90	170	25%	508	75%	678

With the bedding angle as abscissa and the crack percentage as ordinate, the changes of trend of the two kinds of crack content according to the bedding angle can be described as shown in Fig. 12.

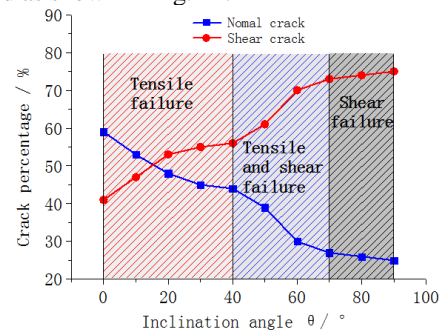


FIGURE 12 Characteristics of crack statistics

Given the information in Fig. 11 and Fig. 12, it can be clearly seen that the angle of the slate-bedding angle can have significant effects on the failure patterns in the specimens of the Brazilian test.

Additionally, from the morphology of the crack connections in the specimens, it is evident the fractures can be divided into 3 categories.

The first fracture type always occurs in specimens with a bedding angle of no more than 40 degrees. The characteristic of this type of fracture is that the percentage of the normal crack and the shear crack are close. The fractures in Fig. 11 (a) - (e) belong to this category. In this type of fracture, the bedding structure has less of an effect on the propagation of the cracks. Although the cracks appear in the layer position, the crack connections in specimens are not dependent on them. The second type of fracture occurs when the bedding angle is greater than or equal to 40 degrees. In Fig. 11 (h) - (j), it can be seen that the percentage of shear cracks is significantly larger than normal cracks. The damage characteristic of this type of fracture is that the specimen is dislocated along the layers and the crack connections are almost all due to the shear cracks. The third type of fracture occurs when the bedding angle is greater than 40 degrees and less than 70 degrees. The distribution of cracks among the specimens fall between the two cases mentioned above; this is the third type of fracture. Both the

bedding dislocations and the crack connections between the layers can be seen as shown in Fig. 11 (g).

Therefore, at the macro level the Brazilian test of slate shows that with a gradual increase in the bedding angle, the fracture of the specimens changed from a purely tensile type to a shear-tension type, eventually becoming a pure shear type.

## 5 Conclusion

Through the use of PFC2D for a simulation of the Brazilian test, the internal stress and strain distribution in the specimens were calculated. The results were consistent with the analytical solution, and the crack initiation and propagation during the test were also displayed from the meso perspective. The results of numerical tests suggest that by increasing the bedding angle, the rock tensile strength shows the characteristics of nonlinear decline. The fracture mode of the specimens had a direct relationship with the bedding angles. When the bedding angle is no more than and

the crack connections in the specimens are not dependent on the cracks at the layer position, the fracture is the tensile type. When the bedding angle is more than and less than and the crack connection depends on the bedding dislocation as well as the cracks between layers, the fracture is the shear-tension type. When the bedding angle is greater than or equal to and the specimens are dislocated along the layers, the fracture is the shear-tension type.

## Acknowledgements

This work was supported financially by the project of the China Postdoctoral Science Foundation (2012M512078) and the National Natural Science Foundation of China (51279073), as well as the Education Department of Henan Province of China (13A560794) and the Science and Technology Department of Henan Province of China (102102310448, 142300410180).

## References

- [1] Chen C 1996 Characterization of deformability, strength, and fracturing of anisotropic rocks using Brazilian tests PH.D. thesis, Dept. of Civil Eng. University of Colorado.
- [2] Debecker B, Vervoort A 2009 Experimental observation of fracture patterns in layered slate *International Journal of Fracture* 159(1) 51-62
- [3] Tavallali A, Vervoort A 2013 Behaviour of layered sandstone under Brazilian test conditions: Layer orientation and shape effects *Journal of Rock Mechanics and Geotechnical Engineering* 5(5): 366-377
- [4] Okubo H 1952 The stress distribution in an anisotropic circular disc compressed diametrically *Journal of Mathematical Physics* 31: 75-83.
- [5] Mahabadi O K, Grasselli G, Munjiza A 2009 Numerical modelling of a Brazilian Disc test of layered rocks using the combined finite-discrete element method Proceedings of the 3rd CANUS Rock Mechanics Symposium, Toronto
- [6] Mclamore R, Gray K E 1967 The mechanical behavior of anisotropic sedimentary rocks *Journal of Manufacturing Science and Engineering* 89(1): 62-73.
- [7] Tavallali A, Vervoort A 2010 Failure of layered sandstone under Brazilian test conditions: effect of micro-scale parameters on macro-scale behaviour *Rock Mechanics and Rock Engineering* 43(5): 641-653
- [8] Potyondy D, Autio J 2001 Bonded-particle simulations of the in-situ failure test at Olkiluoto American Rock Mechanics Association
- [9] PFC2D Version 3.1 User Manual 2004 Minneapolis, MN, USA: Itasca Consulting Group, Inc
- [10] Jianhong Y, Wu F Q, Sun J Z 2009 Estimation of the tensile elastic modulus using Brazilian disc by applying diametrically opposed concentrated loads *International Journal of Rock Mechanics and Mining Sciences* 46(3): 568-576
- [11] Press F 2004 *Understanding Earth* Macmillan
- [12] Claesson J, Bohlooli B 2002 Brazilian test: stress field and tensile strength of anisotropic rocks using an analytical solution *International Journal of Rock Mechanics and Mining Sciences* 39(8): 991-1004.
- [13] Suggested methods for determining tensile strength of rock materials: International Society for Rock Mechanics, Commission on Standardisation of Laboratory and Field Tests *International Journal of Rock Mechanics and Mining Sciences & Geomechanics* 1978 15(6) 99-103
- [14] Tavallali A, Debecker B, Vervoort A 2007 Evaluation of Brazilian tensile strength in transversely isotropic sandstone International Society for Rock Mechanics
- [15] Simpson N, Stroisz A, Bauer A, et al 2014 Failure Mechanics Of Anisotropic Shale During Brazilian Tests 48th US Rock Mechanics/Geomechanics Symposium
- [16] Tavallali A, Vervoort A 2008 Failure of transversely isotropic rock material: effect of layer orientation and material properties Proceedings of the 6th international symposium on ground support in mining and civil engineering construction

Authors	
	<p>&lt; Bing Xie &gt;, &lt;1978.02&gt;,&lt; Luoyang, Henan Province, P.R. China &gt;</p> <p><b>Current position, grades:</b> the Associate Professor of Civil Engineering Department, Luoyang Institute of Science and Technology, China.  <b>University studies:</b> received PHD. from Institute of Rock and Soil Mechanics, Chinese Academy of Sciences.  <b>Scientific interest:</b> His research interest fields include rock mechanics and rock engineering.  <b>Experience:</b> He participated in many research projects about rock mechanics from 2005 to 2014, mainly responsible for modeling work.</p>
	<p>&lt; Yunling Ma &gt;, &lt;1977.06&gt;,&lt; Luoyang, Henan Province, P.R. China &gt;</p> <p><b>Current position, grades:</b> the Associate Professor of Civil Engineering Department, Luoyang Institute of Science and Technology, China.  <b>University studies:</b> received M.Sc. from Xi'an University of Architecture and Technology in China.  <b>Scientific interest:</b> Her research interest fields include rock mechanics and construction material.  <b>Experience:</b> She has teaching experience of over 10 years, has completed several scientific research projects.</p>
	<p>&lt; Wuxiu Ding &gt;, &lt;1970.04&gt;,&lt; Luoyang, Henan Province, P.R. China &gt;</p> <p><b>Current position, grades:</b> the Professor of Civil Engineering Department, Luoyang Institute of Science and Technology, China.  <b>University studies:</b> received PHD. from Institute of Rock and Soil Mechanics, Chinese Academy of Sciences.  <b>Scientific interest:</b> Her research interest fields include rock mechanics and rock engineering.  <b>Experience:</b> She was director of several scientific research program.</p>